Energy, Mines and Resources Canada | Énergie, Mines et Ressources Canada

CANMET

Canada Centre for Mineral and Energy Technology | Centre canadien de la technologie des minéraux et de l'énergie

STRENGTH OF A MINE PILLAR AT COPPER CLIFF SOUTH MINE

G. Herget, P. Oliver, M. Gyenge and Y.S. Yu
Rock Mechanics Laboratory

June 1983

This document is an unedited interim report prepared primarily for discussion and internal reporting purposes. It does not represent a final expression of the opinion of the Canada Centre for Mineral and Energy Technology (CANMET)

Ce document est un rapport provisoire non-révisé et rédigé principalement pour fin de discussion et de documentation interne. Il ne représente nullement l'expression définitive de l'opinion du Centre canadien de la technologie des minéraux et de l'énergie (CANMET)

MICROMEDIA
JAN 20 1984

39 pp

MINERAL RESEARCH PROGRAM
MINING RESEARCH LABORATORIES
DIVISION REPORT MRP/MRL 83-47(TR)

STRENGTH OF A MINE PILLAR AT COPPER CLIFF SOUTH MINE

by

G. Herget*, P. Oliver**, M. Gyenge* and Y.S. Yu*

SUMMARY

Estimates of in situ rock strength are determined as input data for modelling pillar recovery in the 830 orebody of Copper Cliff South Mine. The mineralized medium grained biotite-amphibolite-quartz diorite orebody (O/B) and the adjacent hanging wall (H/W) and footwall (F/W) strata are described according to the CSIR geomechanics classification and the NGI tunnelling index. Both provide a rock mass rating for the ore of 72-79 out of a total of 100 (very good rock). H/W and O/B have similar strengths with F/W strata a little lower.

The intact rock strength for ore at the scale of pillar dimensions is estimated from laboratory tests on samples of 4.1 to 24.1 cm by an inverse strength/sample diameter relationship and the minimum strength available in the orebody (lower bound) is estimated from post peak strength values obtained under triaxial conditions.

As no major through-going geological faults exist in the orebody, the in situ rock strength is estimated to be the average of the lower and upper bound values. A similar value is obtained by applying the percentage rock mass rating to the extrapolated intact rock strength. The unconfined strength of the 826.5 pillar is thus estimated at 66 MPa. Maximum stress determined in the pillar by overcoring is 62.6 MPa.

Stress determinations show that the major stress transfer occurs across the pillars in E-W direction and field stresses after mining indicate a clockwise rotation of 23° from approximately WSW-ENE to E-W.

Field stress determinations fit the range of data observed for northern Ontario. The pillar stress determinations show a reduction of normal stresses at right angle to the pillar wall but there is no stress increase of significance for the vertical or the E-W direction.

---

*Research Scientists, Mining Research Laboratories, Canada Centre for Mineral and Energy Technology, Ottawa, Ontario.

**Rock Mechanics Supervisor, INCO Metals Company, Copper Cliff, Ontario.

RÉSISTANCE D'UN PILIER DANS LA MINE COPPER CLIFF SOUTH

par

G. Herget*, P. Oliver**, M. Gyenge* and Y.S. Yu*

SOMMAIRE

On a déterminé la résistance de la roche emplace qui servira de donnée pour modeller la récupération de piliers du gisement 830 de la mine Copper Cliff South. On décrit le gisement (O/B) de diorite biotite-amphibolite-quartz minéralizé de grains moyens et les couches adjacentes de l'éponte inférieure (F/W) et supérieure (H/W) selon le classement géomécanique CSIR et l'indice NGI pour le percement de tunnel. Les deux permettent d'obtenir l'évaluation de la masse rocheuse du minerai de l'ordre de 72 à 79 sur un total de 100 (très bonne qualité de roche). Les résistances du H/W et du O/B sont du même ordre, cependant celle de la couche F/W est légèrement moindre.

La résistance maximale du minerai intact est évaluée à l'échelle des dimensions d'un pilier par des essais en laboratoire à partir d'échantillons de 4,1 à 24,1 cm, à l'aide d'une relation inverse résistance/diamètre de l'échantillon et la résistance minimale disponible dans le gisement (limite inférieure) à partir de valeurs de résistance post maximale sous des conditions triaxiales.

Comme il n'y a pas de failles qui coupent entièrement le gisement, on calcule la résistance de la roche emplace comme la moyenne des valeurs des

---

*Chercheurs scientifiques, Laboratoires de la recherche minière, Centre canadien de la technologie des minéraux et de l'énergie, Ottawa, Ontario.
**Chef de rayon de la mécanique des roches, INCO Metals Company, Copper Cliff, Ontario.

limites inférieure et supérieure. On ob ient une valeur similaire en appliquant le pourcentage de l'évaluation de la masse rocheuse à la résistance extrapolée de la roche intacte. La résistance non-confinée du pilier 826,5 est évaluée à 66 MPa. La contrainte maximale mesurée dans le pilier par surcarottage est de 62,2 MPa.

Les contraintes de terrain obtenues correspondent à la fourchette des données recueillies dans le nord de l'Ontario. Les contraintes exercées sur le pilier indiquent une réduction contraintes normales perpendiculaire au mur du pilier cependant il n'y a pas d'augmentation importante de contrainte dans la direction verticale ou est-ouest.

CONTENTS

	Page
SUMMARY	i
SOMMAIRE	ii
INTRODUCTION	1
GEOLOGY AND ROCK MASS CLASSIFICATION	1
Geological Setting	1
Rock Mass Classification	2
IN SITU ROCK STRENGTH AND DEFORMATION PROPERTIES	6
Sampling and Testing	6
In Situ Rock Strength	9
In Situ Deformation Properties	13
STRESS DETERMINATIONS	14
Magnitude of Field Stresses	15
Magnitude of Pillar Stresses	17
Orientation of Principal Stresses	18
ACKNOWLEDGEMENTS	19
REFERENCES	20
PROJECT REPORTS	21
APPENDIX A	22

FIGURES

No.		
A1 - A3	Location of stress determinations	

TABLES

No.		
1.	CSIR geomechanics classification for 830 O/B, CCS Mine	5
2.	NGI tunnelling index for 830 O/B, CCS Mine	5
3.	Summary of rock properties	8
4.	Triaxial strength tests on 5.4 cm samples in MPa	9
5.	Calculation of regression based on 43 observations	11
6.	Comparison of field stresses	16
7.	Comparison of stress invariants	17
8.	Comparison of normal stress components (MPa) for 826.5 pillar	18
A1 - A3	Strain recovery, borehole details and ground stresses for Copper Cliff South Mine	23

INTRODUCTION

One aspect of improving productivity in mining operations is to refine our capability of predicting ground behavior. This is required to make better choices of mining method, support systems, backfill procedures and mining layouts. Benefits are improved conservation of the resource base and competitiveness of the mining industry.

In hard rock mines with steeply dipping orebodies blasthole open stoping has the advantage of a low cost per ton ratio and that no workers are required in the stopes. This removes potential accidents from fall of ground and the need for installation of cyclic support.

Below 1000 m, ground pressures are generally high and blasthole open stoping is replaced by more expensive cut-and-fill mining for ground control purposes. However, the potential exists that blasthole open stoping with delayed backfill can be applied successfully at depth if ground behavior can be predicted in advance.

To check our capability in predicting ground behavior for blasthole open stoping operations, the 830 orebody of Copper Cliff South Mine of INCO Ltd., Sudbury/Ontario was chosen for the assessment of in situ rock strength, ground stresses and pillar stability. This was to be checked against ground behavior during mining of the 826.5 pillar.

In the following report the initial effort of determining rock strength, and ground stresses is described.

GEOLOGY AND ROCK MASS CLASSIFICATION

GEOLOGICAL SETTING

The Copper Cliff South mine is located about 6 km WSW from Sudbury at the south rim of the Sudbury Irruptive. The mine is classified as an offset mine because the ore is located a considerable distance from the main felsite/norite contact. All the ore is contained in a quartz diorite dike (medium grained biotite-amphibolite-quartz diorite) which extends south from the norite. The quartz diorite dike is located in Archean metasediments and dissected by a number of trap dikes. The Copper Cliff South mine comprises various lenticular orebodies which are associated with either faults, brecciation or a tendency to fold (1). The present study concentrates on the 830 O/B

which has a general N-S strike and a dip of 65°W. The orebody has a horizontal extension of 365 m and a vertical dimension of 275 m. A longitudinal- and cross-section of the 830 O/B is shown in Fig. 1.

ROCK MASS CLASSIFICATION

Engineering geological mapping was carried out at selected points in the hanging wall (H/W), orebody (O/B), and footwall (F/W) to provide essential background information for detailed rock mechanics investigations.

Information was collected to satisfy the requirements of the NGI Tunnelling Index and the CSIR geomechanics classification. This provided a relative rating of the rock mass in the area of the 830 O/B.

The CSIR Geomechanics classification is based on (2):

1. strength of intact rock material,
2. drill core quality (RQD),
3. condition of joints,
4. spacing of joints, and
5. groundwater.

According to the magnitude of the ratings one of five rock mass classes can be selected. The ratings range from <20 to 100.

The NGI Tunnelling Index is calculated from (3):

1. rock quality designation (RQD),
2. joint set number (Jn),
3. joint roughness number (Jr),
4. joint alteration number (Ja),
5. joint water reduction factor (Jw), and
6. stress reduction factor (SRF).

A quality index (Q) is calculated as follows:

$$Q = \left(\frac{RQD}{Jn}\right) \times \left(\frac{Jr}{Ja}\right) \times \left(\frac{Jw}{SRF}\right)$$

Q values range from 0.001 to 1000. For the interested reader details are also given in Ref. 4.

In both classifications RQD values occupy a prominent position. RQD values are usually obtained from NX drill core which was not available. To obtain the required information, a procedure by Priest and Hudson (5) was used which is based on the recording of fractures intersected by underground drift walls. The fracture spacing is used to determine the negative exponential distribution of per cent frequency of discontinuity spacing x in terms of the average number of discontinuities per metre, λ.

$$f(x) = \lambda\, e^{-\lambda x}$$

This in turn was used to calculate RQD values. The drifts possessed a height of 3.65 m (12 feet) and the composite plot in Fig. 2-A shows observations plotted in intervals of 0.15 m. A list of observations and statistical values is given below to characterize hangingwall (H/W), footwall (F/W) and orebody (O/B).

Fracture Data	Location: H/W	O/B	F/W
Number of discontinuities (n)	32	211	221
Length of scan line	12.6 m	56.8 m	90.2 m
Mean spacing (S_m)	0.39 m	0.27 m	0.41 m
Discontinuities/m (λ)	2.54/m	3.71/m	2.45/m
Regression coefficient (a)	-0.39	-1.27	-.76
Intercept (b) (see Fig. 2)	1.12	1.52	1.29
Correlation coefficient (r)	0.61	0.96	0.93
RQD	97%	95%	98%

For the orebody and footwall the data base was adequate and a good fit of the observed fracture spacings to a negative exponential distribution was obtained. Thus RQD was calculated according to (5):

$$RQD = 100\, e^{-0.1\lambda}(0.1\lambda + 1)$$

The joint set number was determined by underground measurements of fracture orientation with a Breithaupt Clar compass. On 1250, 1500 and 1750 levels a total of 475 discontinuities were measured as shown for H/W, O/B, and F/W on contoured equal area nets in Fig. 2-B, C, and D.

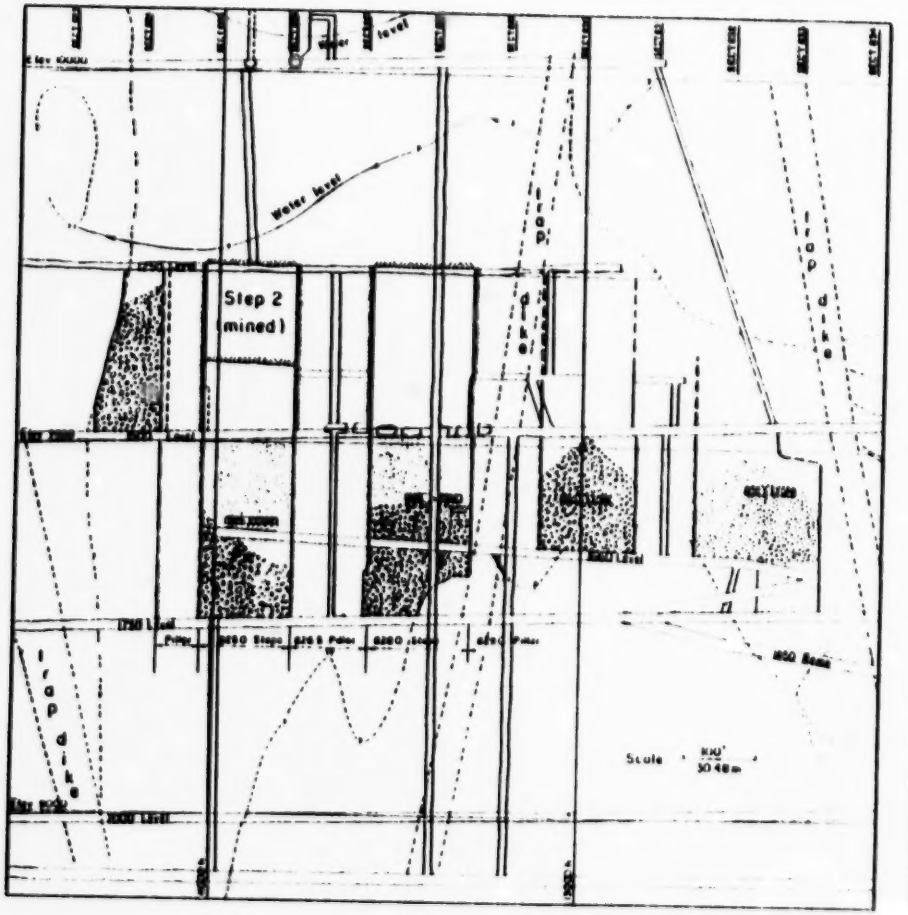

(A)

Fig. 1 (A) - Longitudinal section of 830 ore body through 826.5 pillar (May, 1981).

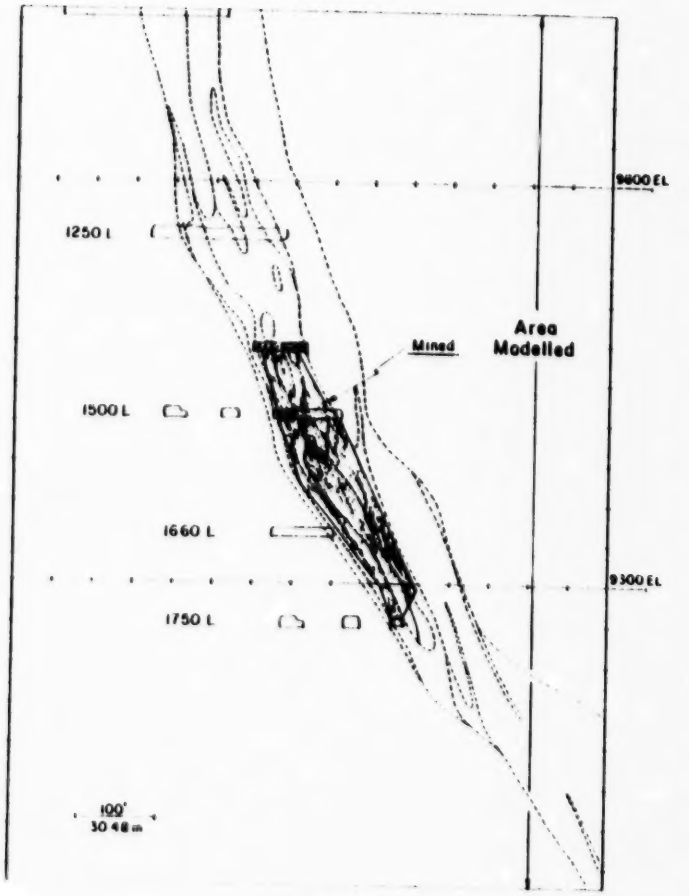

(B)

Fig. 1 (B) - Cross-section of 830 ore body.

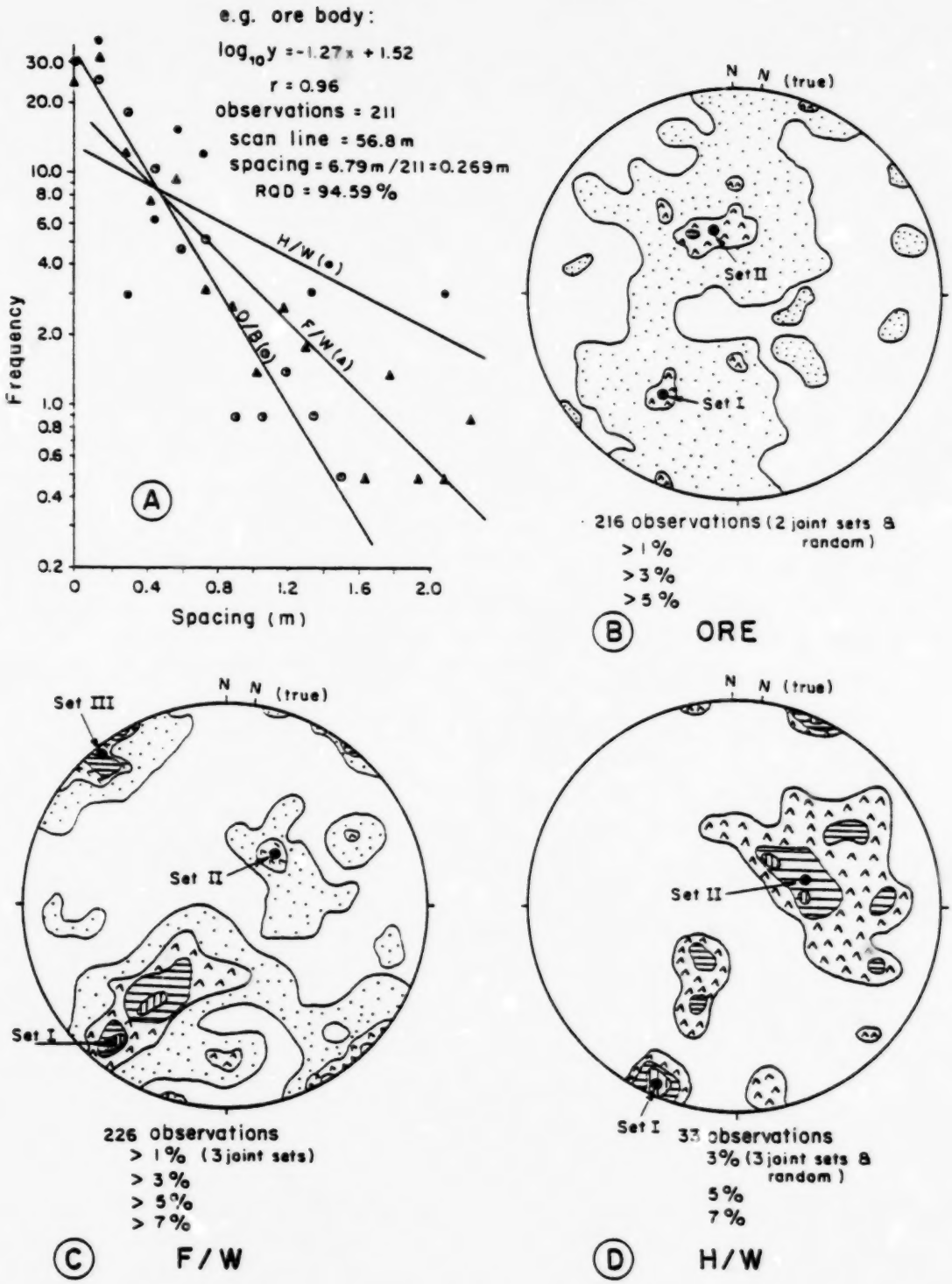

Fig. 2 - Fracture spacing (A) and orientation (B)-Orebody, (C)-Footwall and (D)-Hanging wall.

The individual plots showed the following discontinuity concentrations given by dip direction and dip angle in relation to true north (8°W declination).

	Observations	Set 1	Set 2	Set 3	Random
H/W	33	033/95	258/30	-	few
O/B	216	043/50	173/25	-	few
F/W	226	046/75	236/27	145/80	few

An attempt was made to obtain more information in the hanging wall, but no suitable exposures were available.

All other items to be obtained for the rock mass classification were based on judgements made on site according to references (2,3).

Tables 1 and 2 summarize the values obtained for both rock mass classifications based on discontinuity mapping and underground observations.

According to Table 1 the rock mass in the H/W would be classified as "very good rock" and the O/B and F/W strata are classified as "good rock" which suggests according to the classification the following properties:

	H/W	O/B, F/W
rock mass cohesion (C):	>300 kPa	200-300 kPa
rock mass friction (Ø):	>45°	40-45°
average stand up time:	10 years for 5 m span	6 months for 4 m span

The strength values are rather low because the above values translate into a uniaxial compressive strength (Q_o) of >1.5 MPa for the H/W and 0.9 - 1.5 MPa for the orebody and footwall on the basis of a straight line Mohr's envelope:

$$Q_o = \frac{2\ C \cos \phi}{1 - \sin \phi}$$

The value of the classification however lies more in defining a relative rock strength rating.

Table 1 - CSIR geomechanics classification for 830 O/B, CCS Mine

Parameter:	Rock strength (MPa)	RQD (%)	Joint spacing (m)	Joint condition	Groundwater	Rock Mass Rating (RMR) Maximum 100
Location						
H/W	100-200	90-100	0.39	*	Moist	
Rating	12	20	20	20	10	82
O/B	100-200	90-100	0.27	*	Moist	
Rating	12	20	10	20	10	72
F/W	100-200	90-100	0.41	*	<25L/min	
Rating	12	20	20	20	7	79

*hard joint wall rock <1 mm separation.

Table 2 - NGI tunnelling index for 830 O/B, CCS mine

Parameter	RQD %	Jn (Joint number)	Jr (rough-ness)	Ja (alter-ation)	Jw (water)	SRF (stress reduc-tion)	Q (Quality Index)	RMR Equiv-alent
Location								
H/W	97.3	6	3	1.00	1.0	1.0	49	79
O/B	94.6	6	3	1.00	1.0	1.0	47	79
F/W	97.4	12	3	1.00	1.0	1.0	24	73

In Table 2 the rock is also classified as "good" to "very good" with Q-values of 24 to 49. The rock appears to be weakest in the footwall.

A comparison with the CSIR Rock Mass Rating (RMR) is possible by (2):

$$RMR = 9 \cdot \log_e Q + 44$$

This provides the Q values in terms of the CSIR geomechanics classification as 73 to 79 for the footwall to hanging wall strata. Both classifications suggest a rating for the orebody of 72 to 79 out of a maximum of 100.

IN SITU ROCK STRENGTH AND DEFORMATION PROPERTIES

To obtain quantitative information on rock strength and deformation parameters, samples were obtained for uniaxial and triaxial compressive strength testing.

SAMPLING AND TESTING

Sampling was carried out by diamond drilling at various locations of Copper Cliff South Mine as given below. The different sizes were obtained to make a judgement on the size effect for strength and deformation modulus.

Orebody:

Core diameter (cm)	No. of samples	Location + Direction of Drilling	Hole No.
4.1 (BX)	10	1250 level, 15695N/21870E Drilling West	CCS6
5.4 (NX)	10		CCS7
14.4	4		CCS8
24.1	13		
14.4	6	1500 level, Stn 1	CCS13
Footwall			
5.4 (NX)	10	1500 level, 15710N/21940E Drilling East	CCS10
Hanging Wall			
5.4 (NX)	10	1500 level, 15665N/21645E Drilling West	CCS11
Trap Dike			
5.4 (NX)	10	1500 level, 15900N/21885E Drilling West	CCS12

All cylindrical samples were cut to a height/diameter ratio of 2.0 and the ends were prepared with a parallelism of better than 0.001D. Twelve Brazilian disc tests were carried out on the 5.4 cm diameter ore material with a thickness of 2.7 cm. A summary is given in Table 3.

Triaxial strength tests were carried out at confining pressures of 1.03 MPa, 3.45 MPa and 10.34 MPa and yielded the mean value given in Table 4. After loading the NX-ore samples under triaxial condition to failure, the axial stress was reduced until the sample stabilized and by maintaining the confining pressure, axial stress was increased until slippage or failure occurred. This produced the strength value for the fractured specimen.

The mean values are plotted in Fig. 3 and for the rather narrow range of confining pressures, a straight line envelope provides a good fit for the intact samples with an angle of internal friction of 58.5°. The Hoek and Brown (4) relationship for σ_1/σ_3 provides a less good fit but is probably more realistic in the case of larger confining pressures. For the fractured samples a mean failure envelope is defined by an angle of internal friction of 49°. Due to the interlock of fracture surfaces, the stability of fractured samples does not rely on friction because asperity interlock provides shear strength at zero normal stress (apparent cohesion).

For a straight line envelope the stresses at failure are:

$$\sigma_1 = Q_o + j\,\sigma 3$$

$$Q_o = \frac{2\,C\cos\phi}{1-\sin\phi}$$

$$j = \frac{1+\sin\phi}{1-\sin\phi}$$

with Q_o = uniaxial compressive strength
C = cohesion
ϕ = internal angle of friction.

This allows to calculate a value for apparent cohesion (C) and the uniaxial strength of a fractured sample:

$$j_{49°} = \frac{1+\sin 49°}{1-\sin 49°} = 7.163$$

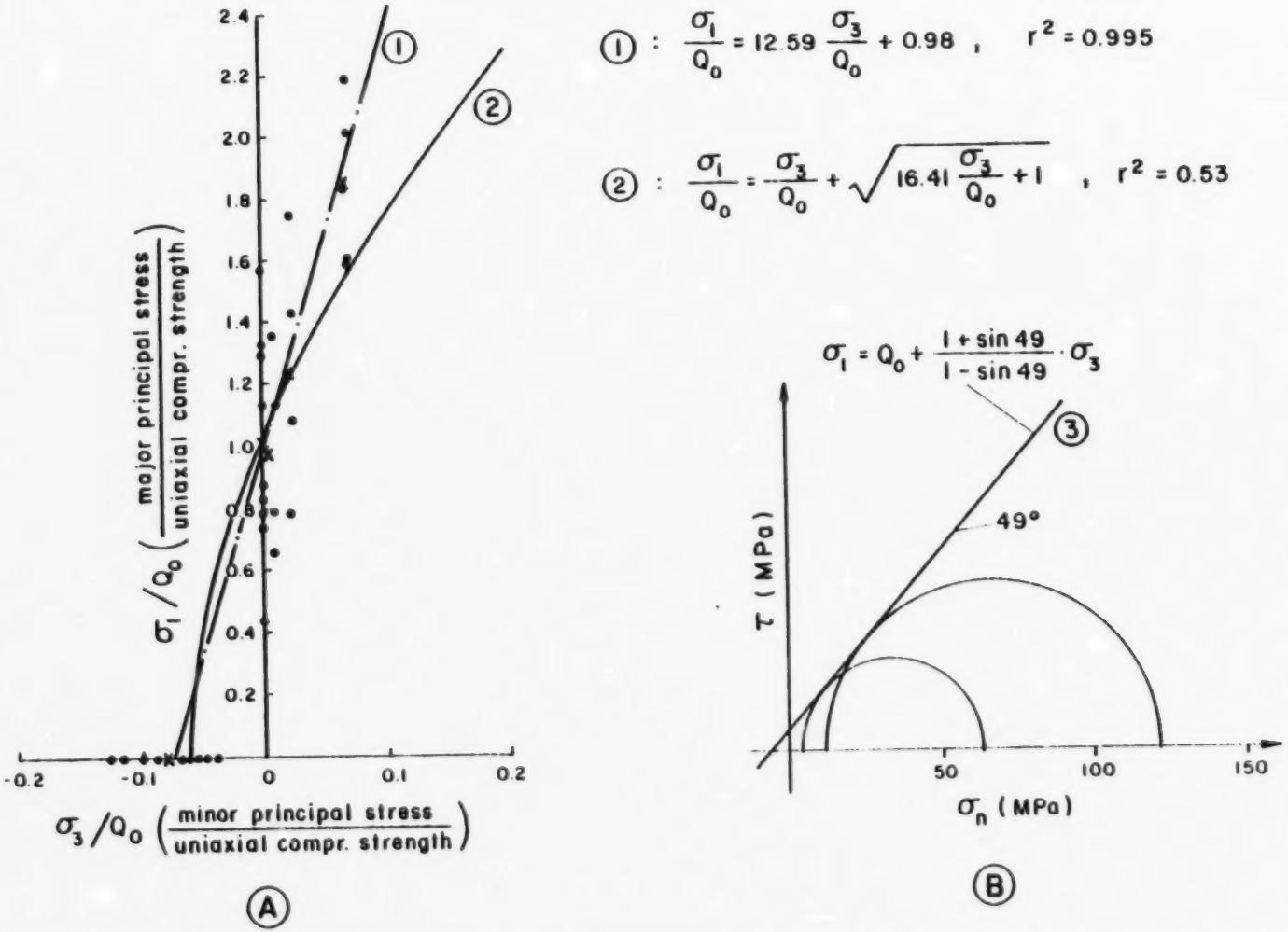

Fig. 3 - Triaxial strength of intact (A) and fractured (post peak) (B) ore samples (X = mean values of observations. (1) straight line approximation, (2) Hoek and Bray Formula, (3) mean strength of fractured samples.

Table 3 - Summary of rock properties

Material	Sample Diameter cm (in.)	Uniaxial strength MPa (10^3 psi) Mean	St. Dev.	E-modulus GPa (10^6 psi) Mean	St. Dev.	Tensile strength σ_t, MPa (psi) Mean	St. Dev.	Poisson's ratio ν Mean	St. Dev.	Density ρ, g/cm^3 (lb/ft^3) Mean	St. Dev.
	4.1	186.2	45.5	88.9	3.4			0.267	0.005	2.99	0.09
	(1 5/8)	(27.0)	(6.6)	(12.9)	(0.5)					(186.6)	(5.6)
Number of tests (n):		10		3				3			
	5.4	154.8	49.8	77.2	3.4	12.32	3.80	0.270	0.010	3.25	0.36
	(2 1/8)	(22.4)	(7.2)	(11.2)	(0.5)	(1787)	(551)			(202.8)	(22.5)
Number of tests:		10		3		12		3			
	14.4	114.6	48.7	75.7	9.6			0.280	0.010	2.93	0.07
Ore											
	(5 5/8)	(16.6)	(7.0)	(10.9)	(1.4)					(182.8)	(4.4)
Number of tests:		10		5				2			
	24.1	86.2	15.9	72.4	1.4			0.260	0.040	3.21	0.22
	(9 1/2)	(12.5)	(2.3)	(10.5)	(0.2)					(200.3)	(13.7)
Number of tests:		13		5				5			
	5.4	151.7	36.5	74.5	2.8			0.275	0.040	2.73	0.03
Footwall											
	(2 1/8)	(22.0)	(5.3)	(10.8)	(0.4)					(170.4)	(1.9)
Number of tests:		10		3				3			
	5.4	126.9	42.1	95.1	4.1			0.263	0.009	2.93	0.01
Trap											
	(2 1/8)	(18.4)	(6.1)	(13.8)	(0.6)					(182.8)	(0.6)
Number of tests:		10		3				3			

Table 4 - Triaxial strength tests on 5.4 cm samples in MPa

Confining pressure	Axial stress at failure	
	Intact samples (n)	Fractured samples (n)
1.03	151.9 ± 48.8 (5)	- (0)
3.45	194.8 ± 56.6 (5)	61.6 ± 7.3 (3)
10.34	287.3 ± 40.2 (5)	120.7 ± 14.6 (2)

$$Q_{o_{3.45}} = \sigma_1 - j\,\sigma_3 = 61.6 - 7.163 \times 3.45 = 36.88 \text{ MPa}$$

$$Q_{o_{10.34}} = \sigma_1 - j\,\sigma_3 = 120.7 - 7.163 \times 10.34 = 46.63 \text{ MPa}$$

$$\text{Mean } Q_o = 41.8 \text{ MPa}$$

$$C = \frac{Q_o(1 - \sin\phi)}{2\cos\phi} = \frac{20.9 \times 0.245}{0.656} = 7.8 \text{ MPa}$$

IN SITU ROCK STRENGTH

From earlier work on Elliot Lake quartzite, Wawa siderite and Timmins andesite/diorite it appeared to be feasible to estimate the in situ rock strength on the basis of an extrapolation of the strength/size decay curve. For this purpose the uniaxial compressive strength tests had been carried out on samples with a constant height/diameter ratio of 2.0 and diameters of 4.1, 5.4, 14.4 and 24.1 cm.

The following uniaxial compressive strength values were obtained in MPa for the various size samples ($\bar{x}$ = mean, s = standard deviation):

4.1 cm: 244.8, 226.8, 222.7, 219.9, 217.9, 187.5, 151.7, 151.0, 146.9, 94.5; $\bar{x}$ = 186.4, s = 45.8

5.4 cm: 245.5, 206.2, 200.6, 175.1, 153.1, 136.5, 128.2, 121.3, 113.1, 68.3; $\bar{x}$ = 154.8, s = 49.8

14.4 cm: 212.4, 160.6, 149.6, 127.0, 124.8, 114.3, 80.8, 66.9, 62.3, 48.2; $\bar{x}$ = 114.6, s = 48.7

24.1 cm: 120.7, 108.2, 103.4, 93.8, 92.4, 84.1, 81.4, 75.2, 73.1, 73.1, 72.4, 69.6, 68.9; $\bar{x}$ = 85.89, s = 15.9.

A plot of the obtained results is given in Fig. 4. Although the scatter of individual observations is large for each size group, the mean strength values show that the strength decreases with an increase in size and that this is accomplished by a decrease in standard deviation.

Observations of a similar kind have been quantified in literature often by a negative exponential distribution which was also applied to the Copper Cliff South Mine results.

From regression the following was obtained:

$$\log Q_o(\text{MPa}) = -0.404 \times \log d\ (\text{cm}) + 2.484$$

with Q_o = uniaxial compressive strength
d = diameter.

This relationship provided a good statistical fit to the range of observed data. However, extrapolation of such a relationship to the size of a pillar provided rather low and very questionable values (12 MPa) for the estimate of pillar strength as shown in Table 5.

Laboratory tests show that the rapid strength/size decay observed in the range of 5 to 25 cm is not maintained as the sample size increases over many orders of magnitude. Field observations of ground stresses, back calculations of pillar strength and the laboratory strength of fractured samples suggest much higher strength values. To satisfy the size effect over many orders of magnitude, it appears that a concept of an asymtotic value of strength (critical strength) is more appropriate.

For the purpose of extrapolation an inverse relationship was applied to the sample data as follows:

$$Q_o = \frac{a}{d\ [\text{cm}]} + C$$

This produced a relationship of

$$Q_o(\text{MPa}) = [\frac{462.3}{d(\text{cm})} + 72.6]\ \text{MPa}$$

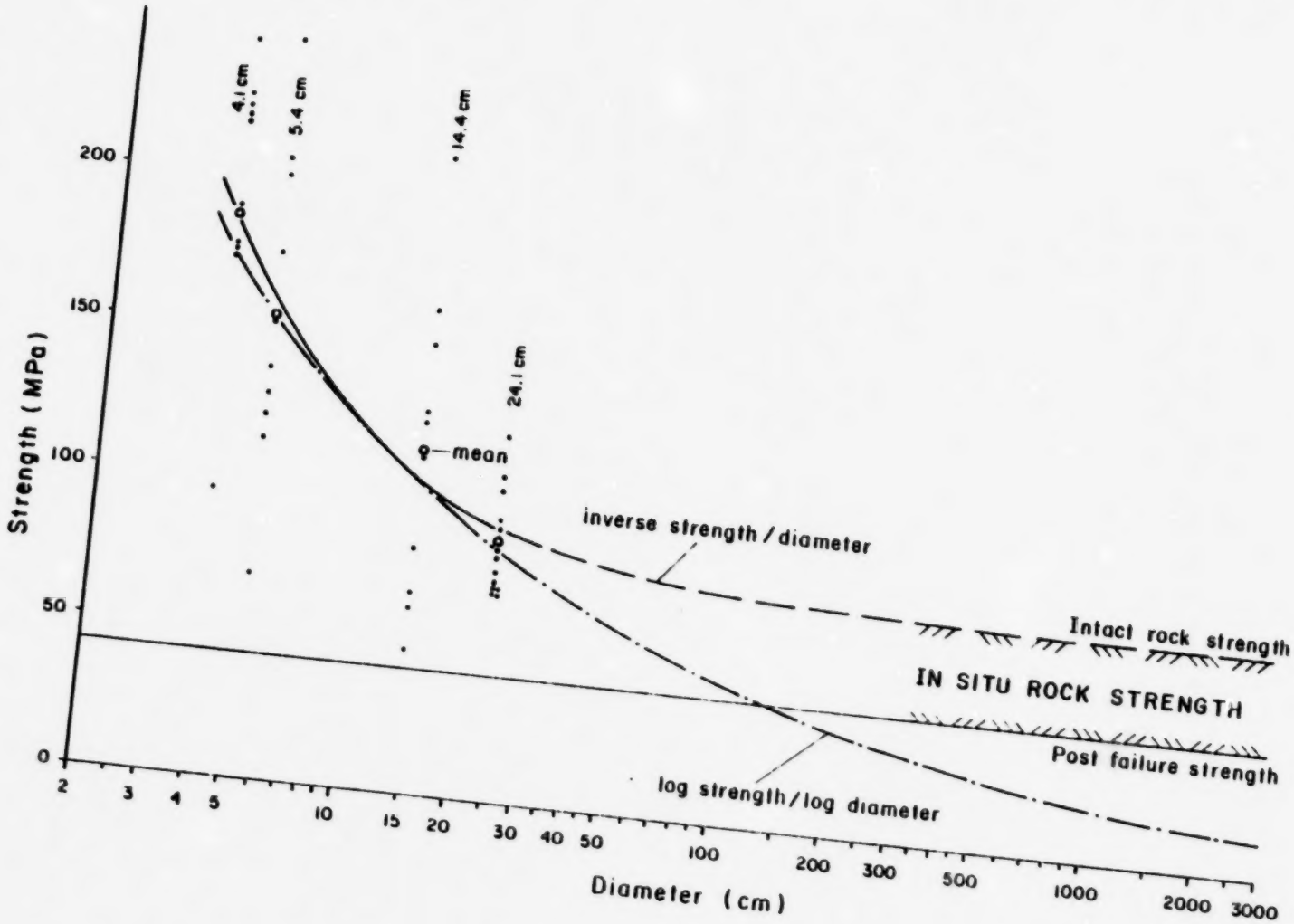

Fig. 4 - Strength/size decay extrapolation.

Table 5 - Calculation of regression based on 43 observations

Diameter [cm]	Observed mean strength [MPa]	Log strength/[1] log diameter	Strength as[2] inverse of diameter
4.1	186.4	172.2	185.3
5.4	154.8	154.1	158.2
14.4	114.6	103.6	104.7
24.1	85.9	84.2	91.8
100	-	47.4	77.2
500	-	24.7	73.5
1000	-	18.7	73.0
3000	-	12.0	72.7
∞	-	0	72.6
slope	-	-0.404	462.317
intercept	-	2.484	72.575
correl. coeff	-	0.457	0.462

[1] Example $\log Q_{100\ cm} = -0.404 \times \log 100\ cm + 2.484 = 1.675$

$$Q_{100\ cm} = 10^{1.675}[MPa] = 47.4\ MPa$$

[2] Example $Q_{100\ cm} = \frac{462.317}{100\ cm} + 72.575 = 77.2\ MPa$

The statistical fit of the inverse relationship is similar to the log strength/log size relationship but provides more meaningful results for the in situ rock strength of intact material as shown in Fig. 4 and Table 5.

The correlation coefficient is in both cases similar and unfortunately relatively low because of the scatter in the sample data.

The extrapolation of a sample base over three orders of magnitude may be precarious and a judgement is necessary on the lower bound in situ strength. The lower bound in situ strength is considered to be presented by a completely fractured pillar which possesses fractures with some interlock (cohesion >0) and horizontal confinement at the hanging wall and footwall contact.

The most suitable equivalent were the post failure strength values of NX core in ore obtained during triaxial testing as shown in Fig. 3-8. The extrapolation to unconfined compressive strength provided a mean value of 41.8 MPa. This value was used as the lower bound of the in situ rock strength of ore-material containing through-going fractures in an orientation favourable for failure.

The in situ rock strength of a pillar, will lie between the strength of the intact material, extrapolated to the relevant size, and the strength of the fractured material.

Depending on the fracturation, the actual in situ rock strength will lie more towards the upper or the lower boundary. For an average condition, e.g. some geological fractures exist but there are no through-going faults favorably oriented for failure, it is assumed that the in situ rock strength is the mean value between the upper and lower bound. Thus for the given dimensions and a pillar with a Width/Height ratio of 0.5 it is suggested 1/2(41.8 + 72.6) MPa = 57.2 MPa.

A similar value is obtained if the orebody rating of 75% from the CSIR classification is applied to the in situ intact rock strength. This yields 72.6 MPa x 0.75 = 54.5 MPa. It appears however, that the value of 57.2 MPa is more reliable. According to Obert and Duvall (6), the strength of pillars (Q_p) increases with an increase of W/H ratio according to

$$Q_p = Q_{\frac{W}{H}=1} (0.778 + 0.222 \frac{W_p}{H_p})$$

If the pillar strength for W/H = 0.5 is 57.2 MPa,

$$Q_{\frac{W}{H}=1} = \frac{57.2 \text{ MPa}}{(0.778 + 0.222 \times 0.5)} = 64.3 \text{ MPa}$$

For the 826.5 pillar the pillar dimensions are for horizontal stress transfer

W_p = N-S width = 30.4 m

H_p = E-W extent = (22.8 m - 30.4 m)/2 = 26.6 m

For the 826.5 pillar $\frac{W_p}{H_p}$ = 1.14 and the strength is thus

$$Q_{P_{826.5}} = 64.3 \quad (0.778 + 0.222 \frac{30.4}{26.6}) = 66.3 \text{ MPa (9620 psi)}$$

IN SITU DEFORMATION PROPERTIES

Deformation moduli were determined with the aid of strain gauges and LVDTs. The following values were obtained in GPa for the different size ore specimen from LVDT measurements:

4.1 cm: 89.6, 92.4, 84.8, $\bar{x} = 88.9 \pm 3.8$

5.4 cm: 81.4, 76.5, 73.1, $\bar{x} = 77.0 \pm 4.2$

14.4 cm: 83.4, 87.6, 73.4, 69.8, 64.5, (44.8, 42.1, 45.4), $\bar{x} = 75.7 \pm 9.6$

24.1 cm: 75.2, 72.4, 72.4, 71.7, 71.0 $\bar{x} = 72.5 + 1.6$

The determination of the deformation moduli of the 14.4 cm samples showed a large variation and the last three values were considered part of a different population on the basis of a t-test.

83.4	44.8	$s(\bar{x})$ = standard dev. of mean
87.6	42.1	$\bar{s}(\bar{x})$ = pooled estimate of the mean
69.8	45.4	obtained from two sets of data
		which give $\bar{x}_1$ and $\bar{x}_2$.
73.4		
64.5		
$\bar{x}$ = 75.7	44.1	
n = 5	3	
s = 9.6	1.76	

$$\bar{s}(x) = \frac{\Sigma(\bar{x}_1 - x_1)^2 + \Sigma(\bar{x}_2 - x_2)^2}{n_1 + n_2 - 2} = \frac{374.84}{6} = 7.9$$

because

$$\Sigma(\bar{x}_1 - x_1)^2 = s_1^2 \cdot (n_1 - 1) = 9.6^2 \cdot 4 = 368.64$$

$$\Sigma(\bar{x}_1 - x_1)^2 = s_1^2 \cdot (n_2 - 1) = 1.76^2 \cdot 2 = 6.20$$

Degrees of freedom 8 - 2 = 6

$$\bar{s}(\bar{x}) = 7.9 \quad \frac{1}{5} + \frac{1}{3} = 5.77$$

Hypothesis $\bar{x}_1 = \bar{x}_2$

$$t = (75.7 - 44.1)/5.77 = 5.48$$

This high t-value indicates that there is less than one chance in a hundred to be wrong when rejecting the hypothesis that both mean values are the same.

The mean values for each size group show a definite size effect and extrapolation to the pillar size was done with an inverse relationship similar to that used for the strength value. This provided the following relationships on the basis of 16 observations:

$$E[GPa] = [\frac{63.94}{d[cm]} + 70.11] \text{ GPa}$$

with a correlation coefficient of r = 0.66.
At a pillar diameter of 3000 cm the elastic modulus would be 70.13 GPa.

In regard to Poisson's ratio no size effect was observed for the 13 samples. A mean value of 0.26 $\pm$ 0.04 was obtained.

STRESS DETERMINATIONS

Stress determinations were carried out in 826.5 pillar and areas away from the influence of mining as shown in the location plans of Fig. A1, A2 and A3. All stress determinations were carried out with the CSIRO triaxial straincell developed by the Commonwealth Scientific and Industrial Research Organization, Australia. The cell is commercially available in North America and the borehole geometry is similar to that used for overcoring of the USBM deformation metre. Details of the procedure are given in literature references (7,8).

All overcored hollow rock cylinders were loaded by a cylindrical hydraulic jacket to determine gauge response (bond quality) and field elastic modulus. This elastic modulus was however, in some cases excessively high and

values from laboratory testing were used to calculate stress magnitudes. It was later discovered that the pressure gauge provided an incorrect read out. All hollow core cylinders were cut to inspect the bond quality (air bubbles, glue distribution). For calculation of ground stress tensors, the program "overcore" was used as supplied by the distributor of the stress determination equipment.

MAGNITUDE OF FIELD STRESSES

Field stresses were determined on 1250 level and 2050 level. Collar positions, borehole directions, rock properties, strain recovery and calculated stresses are given in Fig. A1 - A3 and Tables A1, A2 and A3. All measurements were made in orebody material.

Stress determinations can provide a rather large scatter for individual sites and in general many readings are required to obtain representative field data. From measurements in Northern Ontario, however, good background information existed which allowed a comparison with the obtained Copper Cliff South Mine data.

Generally it has been found for Northern Ontario (9) that σ_3 (minimum principal compressive stress) is vertical and approximates overburden weight. The ratio of average horizontal stress to vertical stress changes with depth according to

$$\sigma_{H_{average}}/\sigma_V = \frac{251.68}{\text{Depth (m)}} + 1.14$$

In addition the change of average horizontal stress with depth is

$$\sigma_{H_{average}} = 9.86 \text{ MPa} + 0.0371 \text{ MPa/m}$$

and for extreme cases:

$$\sigma_{H_{average\ (extreme)}} = 12.36 \text{ MPa} + 0.0586 \text{ MPa/m}$$

Table 6 provides a comparison of field stresses with Northern Ontario data. Results from test 1250-1 are relatively high and have been influenced by some type of stress concentration. Tests 1250-3, 4 and 5 are much lower and give a mean value of stress in vertical direction which is only about 35% above

Table 6 - Comparison of field stresses

Test No.	Depth (m)	σ_V	σ_H (average)	σ_H/σ_V
1250-1	353	29.26	30.11	1.02
1250-3	353	10.54	26.43	2.50
1250-4	353	16.59	31.69	1.91
1250-5	353	13.79	19.97	1.45
Mean, Excluding 1250-1		13.64	26.03	1.91
Northern Ontario (9): average		10.11[1)]	22.91	1.86
extreme		21.29	32.99	
2050-1	600	29.22	41.04	1.40
2050-2	600	15.47	29.63	1.92
2050-3	600	19.66	35.46	1.80
2050-4	600	16.18	32.05	1.98
Mean		20.13	34.52	1.72
Northern Ontario (9): average		17.24	32.12	1.56
extreme		36.18	47.52	(Reference 2)

1) Obtained from overburden weight/m^2 = Mass (kg/m^3) x depth (m) x acceleration (m/s^2)/area(m^2)

$$= \frac{kg}{m \cdot s^2 \cdot m^2} = N/m^2$$

overburden stress. The mean value for σ_V from 2050 level is only 17% above overburden weight.

Good agreement exists in regard to the σ_H/σ_V ratio and the average horizontal stress. Therefore the stress from 1250-3,4,5 and 2050-1,2,3,4 are regarded as acceptable estimates of the in situ stress at Copper Cliff South Mine.

MAGNITUDE OF PILLAR STRESSES

As shown in Tables A1 to A3, pillar stresses were determined on 1250 level (347.5 m) and 1500 level (416.5 m) in the 826.5 pillar of the 830 orebody, Copper Cliff South Mine. To determine whether measured pillar and field stresses are comparable, the first stress invariant (I_1) is calculated for the field and pillar stress tensor.

$$I_1 = \sigma_1 + \sigma_2 + \sigma_3 = \sigma_{E-W} + \sigma_{N-S} + \sigma_V$$

A comparison is given in Table 7 and shows that all field stress values from 1250 level are higher than expected and that result 1250-1 can not be considered representative compared to earlier measurements (9). Pillar stress value 1250-3 also appears to be excessively high.

Table 7 - Comparison of stress invariants

Location	Depth (m)	Test	I_1 (MPa)	I_1/m	Remarks
Pillar Stress Values					
826 pillar	347.5	1250-2	61.78	0.18	high
826 pillar	347.5	1250-3	102.39	0.29	
826 pillar	416.5	1500 F/W-comb.	50.67	0.12	
826 pillar	416.5	1500 H/W-comb.	58.44	0.14	
			Mean:	0.15	
Field Stress Values					
1250	353.3	1250-1	89.50	0.25	high
1250	353.3	1250-3,4,5	65.70	0.19	
2050	600.2	2050-1,2,3,4	89.21	0.15	
			Mean:	0.17/m	
Northern Ontario (9):		Average	Extreme		
	353.0	55.93	87.27	0.16/m (average)	
	600.0	81.48	131.22	0.14/m (average)	

At the mine the average overburden density is 2930 kg/m^3 and standard acceleration is 9.80665 m/s^2. This provides a stress in MPa at a depth of 353 m and 600 m of 10.11 MPa and 17.24 MPa, respectively.

During mining adjoining stopes to a pillar, the confinement of the pillar is less than that of the original ground and a stress redistribution can occur which is not necessarily detected by the comparison of stress invariants. Hanging wall and footwall are bridged by the 826.5 pillar in E-W direction and in Table 8 pillar stress and field stress components are compared in E-W, N-S, and vertical direction.

Table 8 - Comparison of normal stress components (MPa) for 826.5 pillar

Type	Location	Orientation					
		VERT	VERT	N-S	N-S	E-W	E-W
Field stresses	1250 - 3,4,5 (353 m)	13.6		18.8		32.3	
Pillar stresses	1250-2 (347.5 m)		14.8		12.6		34.3

The values in Table 8 indicate that there is a drop of 6.2 MPa from field to pillar stresses in N-S direction as expected due to the loss of confinement. The increase in E-W and vertical stress components from field to pillar stress is however marginal only.

ORIENTATION OF PRINCIPAL STRESSES

Figure 5-A and B display graphically the orientation of principal stress directions for the measured field and pillar stresses. The orientation is relatively stable, but in Fig. 5-A (field stresses) the σ_3 direction is replaced by σ_2 in three out of eight cases. This occurs for the pillar stress determinations only in one out of nine cases.

The 826.5 pillar possesses an E-W orientation and it is interesting to note that compared to the field stress sites the pillar stresses show a rotation of σ_1 by about 23° to line up with the E-W orientation, e.g. maximum stress transfer. It is not anticipated that this change represents a natural variation because field stresses were obtained N and S of the pillar stress sites.

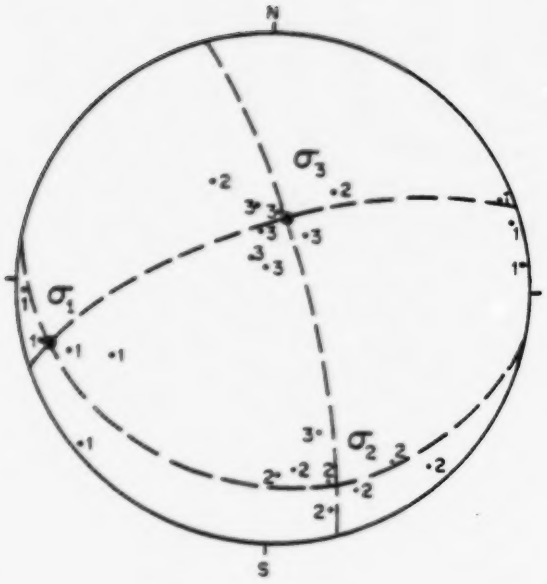

(A) Field

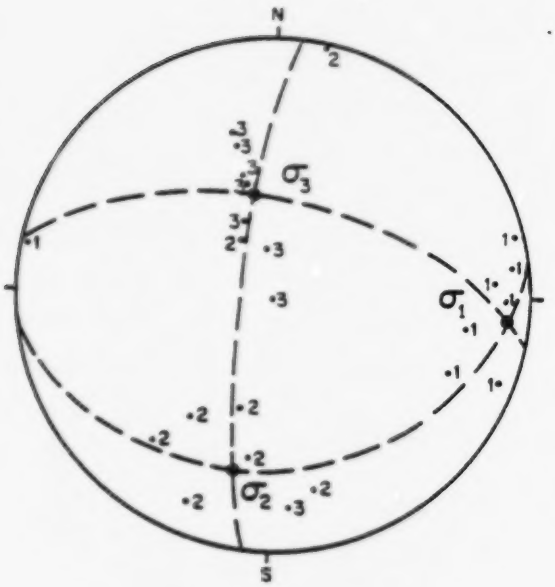

(B) Pillar

Fig. 5 - Principal stress directions for field (A) and pillar (B) stresses in upper hemisphere of equal area net. (Orientation is given as dip direction and dip).

ACKNOWLEDGEMENTS

The authors appreciate the assistance from INCO Metals Company, especially by Mr. Claudio Barsotti, Manager of Research, to carry out this involved field program. Excellent on site cooperation was enjoyed at all times.

REFERENCES

1. Yates, A.B. "Structural geology of Canadian ore deposits"; Symposium Geology Division CIM; Montreal, 596-617; 1948.

2. Bieniawski, Z.T. "Rock mass classification in rock engineering"; Proc Symp on Exploration for Rock Engineering, Johannesburg, vol 1, 97-106; 1976.

3. Barton, N., Lien, R. and Lunde, J. "Engineering classification of rock masses for the design of tunnel support"; Rock Mechanics, vol 6, No. 4, 189-236; 1974.

4. Hoek, E. and Brown, E.T. "Underground excavations in rock"; Institute of Mining and Metallurgy, London, England, 527 p; 1980.

5. Priest, S.D. and Hudson, J.A. "Discontinuity spacings in rock"; Int J Rock Mech Min Sci and Geomech Abstr, vol 14, pp 133-137; Pergamon Press; 1976.

6. Obert, L. and Duval, W.I. "Rock mechanics and the design of structures in rock"; John Wiley & Sons, Inc., 650 p; New York; 1967.

7. Worotnicki, G. and Walton, R.J. "Triaxial 'hollow inclusion' gauges for determination of rock stresses in situ"; Symposium on Investigation of Stress in Rock - Advances in Stress Measurement. The Inst. of Engineers, Australia, National Conference Public. No. 76/4, p. 1-8; 1976.

8. Anon. "Field Manual for CSIRO hollow inclusion gauge"; Geocon Inc., West Lebanon, NH 03784.

9. Herget, G. "Regional stresses in the Canadian shield"; CIM Spec. vol 22, p. 9-16; 13th Canad. Rock Mechanics Symposium, Toronto, 1980

PROJECT REPORTS: COPPER CLIFF SOUTH MINE - NOT PUBLISHED

Herget, G., Gyenge, M., Hedley, D.G.F., Larocque, G., Oliver, P., Yu, Y., Modelling of 830 Orebody of Copper Cliff South, Project Plan. MRP/MRL 81-58(TR)

Yu, Y.S., Toews, N.A. and Wong, A.S., Implementation of Backfill with the MINTAB Program, MRP/MRL 81-62

Yu, Y.S., Toews, N.A., Larocque, G.E., Hedley, D.G.F., Oliver, P. and Herget, G., Modelling of 830 Orebody of Copper Cliff South Mine, INCO: Part 1 - A preliminary assessment using the MINTAB program - MRP/MRL 81-100(TR)

Shama, R., Chodola and Herget, G., Pressure monitoring of mine backfill - MRP/MRL 81-103(TR)

Herget, G., Rock mass classification at Copper Cliff South Mine - MRP/MRL 81-137(TR)

Gyenge, M., Gorski, B. and Shimotani, T. Strength determination of rocks at Copper Cliff South Mine MRP/MRL 82-8(TR)

Herget, G. and Oliver, P., Pillar stress determination at Copper Cliff South Mine, MRP/MRL 82-4(TR).

APPENDIX A

Details on Ground Stress Determination Sites

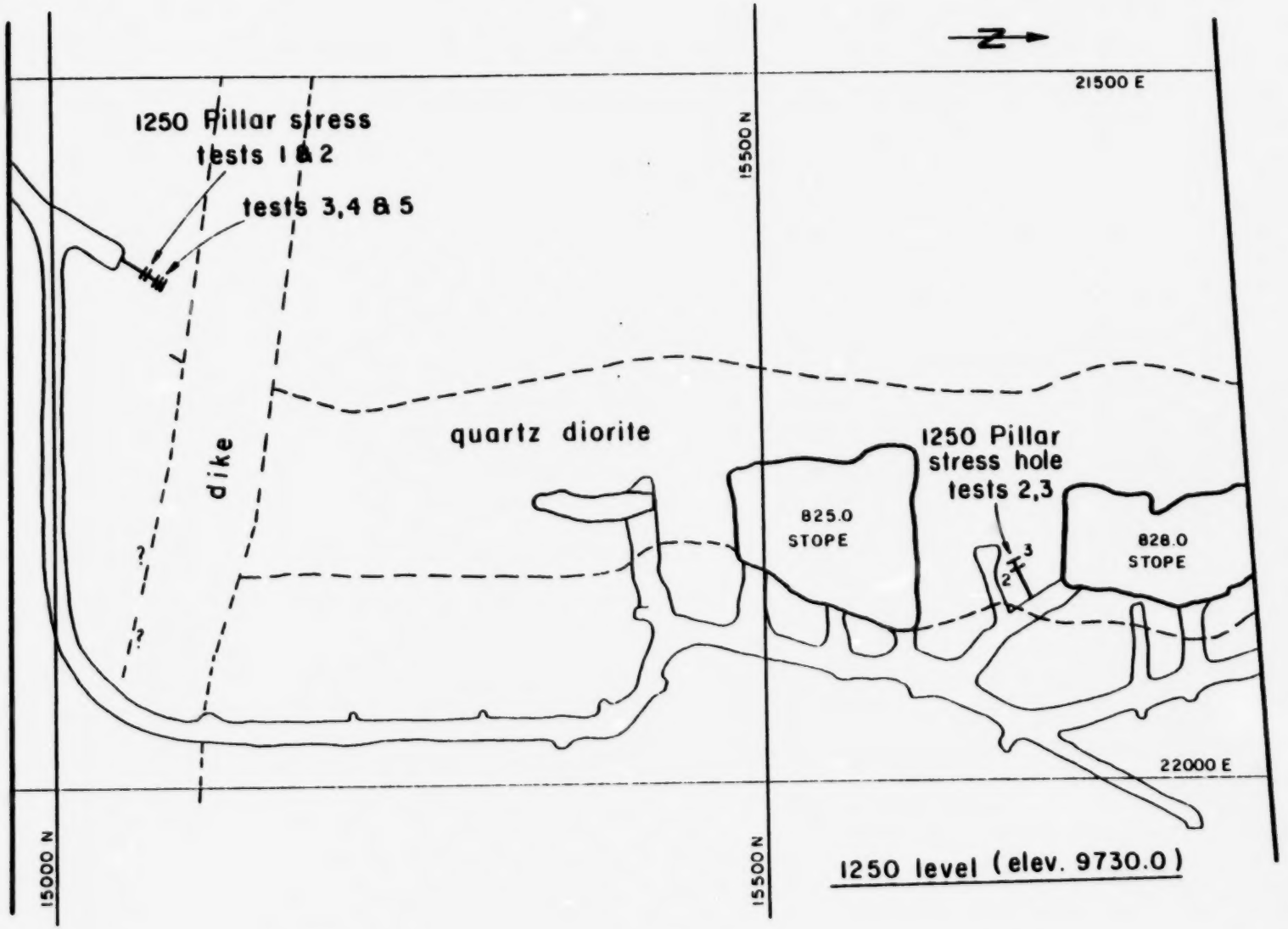

Fig. A1 - Location of stress determinations on 1250 level.

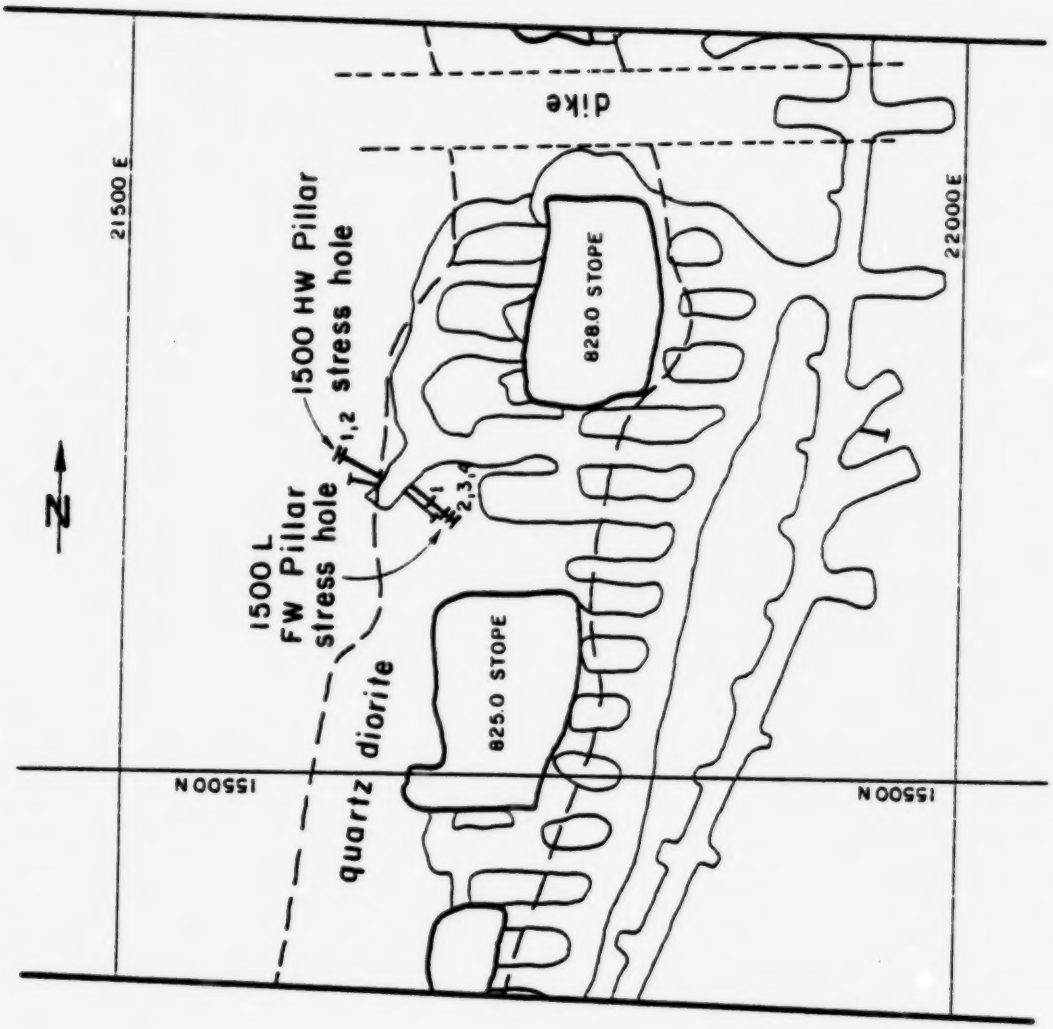

Fig. A2 – Location of stress determinations on 1500 level.

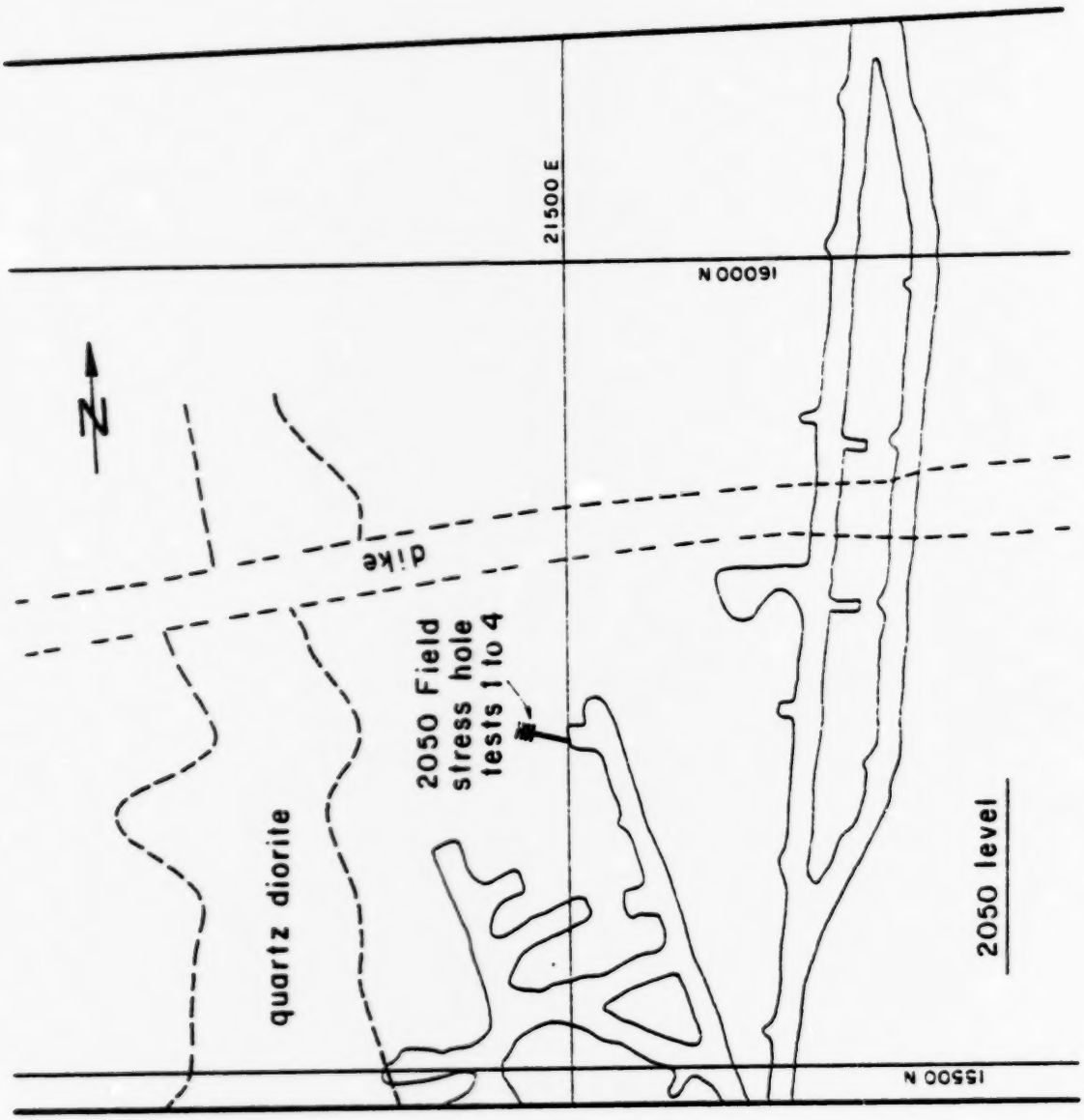

Fig. A3 – Location of stress determinations on 2050 level.

Table A1 - Stress determinations - borehole data and rock properties

Level	Test	Name	Borehole collar co-ordinates			Borehole direction		Date of test		Setting depths					Test quality[3]
			North	East	Depth	AZ	Dip	Setting	Overcore	155 mm	EX	Cell	E[1]	ν[2]	
Field Stresses															
1250	1	1250F1	4587.4	6591.7	353.3	31.7	-4.10	Mar 11/82	Mar 12/82	5.64	6.18	5.89	74.5	0.27	G
	2	1250F2	4587.4	6591.7	353.3	31.7	-4.10	Mar 15/82	Mar 16/82	6.17	6.60	6.38	74.5	0.27	B
	3	1250F3	4587.4	6591.7	353.3	31.7	-4.10	Mar 23/82	Mar 24/82	8.03	8.52	8.27	74.5	0.27	P
	4	1250F4	4587.4	6591.7	353.3	31.7	-4.10	Mar 25/82	Mar 26/82	8.56	9.04	8.76	74.5	0.27	G
	5	1250F5	4587.4	6591.7	353.3	31.7	-4.10	Mar 29/82	Mar 30/82	9.06	9.59	9.26	74.5	0.27	G
2050	1	2050F1	4786.1	6552.7	600.2	285.1	-9.0	Jan 28/82	Jan 29/82	7.33	7.94	7.58	74.5	0.27	G
	2	2050F2	4786.1	6552.7	600.2	285.1	-9.0	Jan 29/82	Feb 1/82	7.92	8.48	8.18	74.5	0.27	G
	3	2050F3	4786.1	6552.7	600.2	285.1	-9.0	Feb 2/82	Feb 3/82	8.47	9.00	8.78	74.5	0.27	G
	4	2050F4	4786.1	6552.7	600.2	285.1	-9.0	Feb 4/82	Feb 5/82	9.03	9.51	9.36	74.5	0.27	G[4]
Pillar Stresses															
1250	2	1250P2	4782.1	6666.4	347.5	246	-2.5	Oct 19/81	Oct 20/81	7.37	7.92	7.47	80.0	0.27	G
	3	1250P3	4782.1	6666.4	347.5	246	-2.5	Oct 21/81	Oct 22/81	8.64	9.19	8.94	80.0	0.27	G
1500	1	1500P11	4776.8	6605.6	416.5	129.5	-9.10	-	Nov 30/81	-	-	5.18	80.0	0.27	G
F/W Hole	2	1500P12	4776.8	6605.6	416.5	129.5	-9.10	-	Dec 3/81	-	-	8.08	80.0	0.27	G
	3	1500P13	4776.8	6605.6	416.5	129.5	-9.10	-	Dec 7/81	-	-	9.24	80.0	0.27	G
	4	1500P14	4776.8	6605.6	416.5	129.5	-9.10	-	Dec 9/81	-	-	9.75	80.0	0.27	G
1500	1	1500P21	4778.0	6600.5	416.5	295.0	-7.40	Dec 24/81	Dec 28/81	8.24	8.84	8.46	74.5	0.27	G
H/W Hole	2	1500P22	4778.0	6600.5	416.5	295.0	-7.40	Dec 29/81	Dec 30/81	8.89	9.59	9.18	74.5	74.5	G

1) Elastic modulus (GPa)

2) Poisson's ratio

3) G (good), P (poor), B (bad)

4) Air bubble observed in glue

Table A2 - Strain recovery measurements, 830 O.B. C.C.S. Mine

Location (level/section)	Test No.	Strain recovery (microinches/inch) 1	2	3	4	5	6	7	8	9	Remarks
Field Stresses											
1250	1	269	985	1106	144	914	650	278	474	285	
820 STA	2	--	--	--	--	--	--	--	--	--	- Core broke through gauges
	3	--	--	350	54	897	851	241	364	600	- Core cracked, gauges 1 & 2 lost
	4	303	292	355	305	841	1023	269	504	477	
	5	206	316	305	130	553	523	175	390	450	
2050	1	312	1023	519	860	635	1178	302	541	546	
827 DD STA	2	292	625	390	743	467	764	318	81	154	
	3	373	712	331	854	429	766	339	249	379	
	4	250	493	280	725	686	1099	328	319	297	- Air bubbles
Pillar Stresses											
1250	2	304	296	490	77	523	289	315	320	365	
826P	3	565	420	635	380	940	522	620	225	548	
1500	1	25	410	-45	600	70	470	100	175	135	
826P	2	97	455	-250	722	-66	416	93	433	442	
F/W hole	3	480	505	-305	770	-155	430	225	510	745	
	4	223	505	-173	1063	-20	780	275	213	246	
H/W hole	1	259	359	292	437	416	591	231	202	204	
	2	245	279	155	500	391	641	215	274	289	

Table A3-I - Ground stress tensors - field stresses

Location (level/section)	Test No.	Normal stress MPa			Shear stress (MPa)			Principal stresses (MPa)								
		Error			Error			Sigma 1			Sigma 2			Sigma 3		
		N-S	E-W	Vert	NS/EW	EW/Vert	NS/Vert	Mag	Azimuth	Dip	Mag	Azimuth	Dip	Mag	Azimuth	Dip
Field stresses																
1250	1	24.85	35.38	29.26	6.93	-9.12	-3.69	44.96	244.7	32.0	23.34	32.2	53.4	21.20	144.5	15.8
820 STA		0.39	0.17	0.17	0.15	0.11	0.21									
"	2	-	-	-	-	-	-	-	-	-	-	-	-	-	-	-
"	3	15.70	37.16	10.54	6.90	1.74	-0.08	39.28	73.7	3.3	13.77	164.3	9.7	10.35	325.2	79.8
		0.15	0.08	0.13	0.09	0.05	0.13									
"	4	25.40	37.97	16.59	3.85	0.15	-2.95	39.08	253.9	1.7	25.27	163.4	18.3	15.62	349.1	71.6
		0.38	0.20	0.20	0.20	0.13	0.23									
"	5	15.32	24.61	13.79	4.50	0.86	0.79	26.53	67.8	4.9	14.02	331.5	51.5	13.17	161.7	38.0
		0.03	0.02	0.01	0.02	0.00	0.02									
Comb.	1-5	19.04	35.19	13.81	4.96	0.24	-1.24	36.59	254.2	0.3	18.01	164.1	16.6	13.43	345.1	73.4
		2.15	1.37	1.33	1.17	0.70	1.38									
2050	1	39.14	42.94	29.22	0.46	-3.34	-4.04	44.21	250.8	17.0	39.92	157.0	12.5	27.17	32.4	68.7
827 DDSTA		0.0	0.0	0.0	0.0	0.0	0.0									
"	2	23.31	35.94	15.47	1.56	0.95	-5.37	36.14	83.4	0.9	25.95	173.9	27.4	12.63	351.7	62.6
		0.05	0.14	0.07	0.05	0.08	0.03									
"	3	25.62	45.29	19.66	0.53	-1.71	-3.63	45.43	267.7	4.1	27.26	175.8	24.7	17.87	6.5	64.9
		0.05	0.20	0.06	0.05	0.07	0.03									
"	4	31.72	32.37	16.18	1.91	0.39	-1.65	34.02	228.9	2.5	30.27	138.6	6.1	15.98	341.5	83.4
		0.39	0.77	0.34	0.34	0.37	0.19									
Comb.	1-3	25.51	39.40	18.08	1.05	-0.04	-5.01	39.48	265.2	1.2	27.95	174.6	26.8	15.56	357.7	63.2
		1.18	2.18	1.34	0.98	1.40	0.69									

Table A3-II - Ground stress tensors - pillar stresses

Location (level/section)	Test No.	Normal stress MPa			Shear stress (MPa)			Principal stresses (MPa)								
		Error			Error			Sigma 1			Sigma 2			Sigma 3		
		N-S	E-W	Vert	NS/EW	EW/Vert	NS/Vert	Mag	Azimuth	Dip	Mag	Azimuth	Dip	Mag	Azimuth	Dip
Pillar stresses																
1250 826P	2	12.63	34.31	14.84	2.77	2.54	1.12	35.01	82.6	7.5	14.74	330.4	70.7	12.03	175.0	17.6
		.04	.08	.04	.04	.04	.03									
826P	3	24.57	59.65	18.17	9.68	2.52	-1.56	62.23	75.7	2.7	23.01	166.9	23.4	17.15	339.6	66.4
		0.23	0.46	0.20	0.25	0.17	0.17									
1500 826P	1	8.17	24.10	10.27	1.68	4.08	-1.71	25.29	85.9	14.7	10.78	194.6	50.7	6.47	345.1	35.4
		0.92	1.01	0.56	0.66	0.59	0.36									
F/W hole																
	2	8.62	29.61	14.11	-0.01	7.85	-8.28	33.35	99.1	25.2	17.17	213.1	40.9	1.82	346.9	38.7
		0.21	0.23	0.13	0.15	0.17	0.08									
	3	17.25	36.11	15.98	-5.66	11.14	-10.97	44.67	113.1	26.9	19.75	217.7	26.4	4.92	344.9	50.7
		0.24	0.26	0.15	0.17	0.15	0.09									
	4	14.53	43.31	13.20	0.17	5.57	-3.32	44.31	90.8	10.2	16.86	188.0	34.5	9.87	346.7	53.6
		0.16	0.24	0.16	0.15	0.16	0.11									
Comb.	1-4	9.89	29.16	11.62	-0.61	6.90	-4.72	31.77	96.1	20.1	13.69	203.00	38.4	5.21	344.9	44.8
		1.61	2.25	1.43	1.37	1.45	0.82									
1500 826P	1	19.84	24.89	12.19	-1.91	1.07	-2.19	25.75	110.5	7.4	19.58	202.2	12.4	11.58	350.3	75.5
		0.06	0.09	0.04	0.05	0.05	0.02									
H/W hole																
	2	20.24	27.00	11.47	-1.36	-0.06	0.23	27.26	281.0	0.4	19.98	11.0	1.5	11.46	177.2	88.5
		0.29	0.46	0.21	0.23	0.24	0.12									
Comb.	1&2	20.21	25.92	12.31	-1.66	1.13	2.18	26.25	106.9	6.9	20.16	198.4	12.3	11.71	348.4	75.9
		0.44	0.77	0.58	0.39	0.61	0.29									

POOR

QUALITY

ORIGINAL